In vitro evaluation of electrospun blends of gelatin and PCL for application as a partial thickness corneal graft

J B Rose[1], L E Sidney[2], J Patient[1], L J White[1], H S Dua[2], A J El Haj[3], A Hopkinson[2], F R A J Rose[1*]

[1]Centre for Biomolecular Sciences, School of Pharmacy, University of Nottingham, NG7 2RD

[2]Academic Ophthalmology, Division of Clinical Neuroscience, University of Nottingham, Queen's Medical Centre Campus, NG7 2UH,

[3]Institute for Science and Technology in Medicine, School of Medicine, Keele University, Stoke-on-Trent, ST4 7QB;

*Corresponding Author: Felicity R A J Rose; **felicity.rose@nottingham.ac.uk**

Running title: PCL/gelatin fibrous scaffolds for applications in cornea repair

Keywords

Corneal stroma, Electrospinning, Keratocytes, Gelatin, Polycaprolactone

ABSTRACT

The advent of innovative surgical procedures utilizing partial thickness corneal grafts has created a need for the development of synthetic implants to recreate corneal stromal tissue. This work evaluates electrospun gelatin and polycaprolactone (PCL) scaffolds as a potential biomaterial suitable for use in regeneration of corneal stromal tissue. Electrospun gelatin has been used for many years in tissue engineering, however, post-production modification, such as crosslinking, is usually required to mechanically strengthen such scaffolds. This paper aims therefore to compare glutaraldehyde (GA) cross-linked electrospun gelatin scaffolds with electrospun blends of gelatin and PCL at different ratios. Scaffolds were fabricated using electrospinning and characterized by scanning electron microscopy, Attenuated Total Reflectance-Fourier Transform Infrared Spectroscopy (ATR-FTIR), and tensile testing. To evaluate biocompatibility, primary human corneal stromal cells (hCSC) were seeded upon the scaffolds to assess adherence, proliferation and phenotype. Results demonstrated that scaffolds fabricated from mixtures of gelatin and PCL showed increased mechanical strength and plasticity compared to scaffolds fabricated from GA cross-linked gelatin alone. In addition, scaffolds fabricated from PCL and gelatin showed comparable support of hCSC adhesion and proliferation. In conclusion, blended mixtures of gelatin and PCL can be considered as an option in the selection of corneal repair materials in the future.

INTRODUCTION

Developments in corneal surgery over the last 15 years have seen a paradigm shift in the way corneal donor tissue is used[1]. Skilled surgeons now have the option to

treat corneal blindness using partial thickness corneal transplantation, a highly effective and safe alternative to full-thickness transplantation[2]. For example, Deep Anterior Lamellar Keratoplasty (DALK), is a procedure in which only the anterior portion of the cornea is removed and replaced with a prepared portion of donor corneal tissue. DALK has been shown to deliver clinical benefits relative to full thickness transplantation including fewer post-operative complications whilst delivering similar refractive outcomes and graft survival rates[3]. The rise of DALK is now driving the development of stromal mimetic alternatives suitable for grafting[4].

The corneal stroma makes up approximately 90% of the cornea and is composed of orthogonally-stacked lamellae of collagen I fibrils separated by proteoglycans and interspersed with a quiescent cell population known as keratocytes[5-6]. A challenge in developing a successful partial-thickness tissue engineered cornea is mimicking this structure which has been accomplished with some success using electrospinning. Control over electrospinning parameters can yield scaffolds with features in the micro to nano scale similar to the native extracellular matrix[7]. Electrospun scaffolds of natural biopolymers for tissue engineering applications have been successfully reported by numerous groups[8-9]. However, reports of protein denaturation post-electrospinning and high cost of goods have limited the translation of such constructs[10]. Gelatin is a natural biopolymer derived from the controlled hydrolysis of collagen and has seen clinical use in a number of medical areas. It has several advantages over collagen, as it can be electrospun without further denaturation, there is less potential for prion transmission and immunogenic and antigenic reactions, and is less expensive[10-11].

Whilst gelatin appears an ideal material for stromal reconstruction, its solubility in aqueous systems requires a level of post-production modification. Glutaraldehyde (GA) has been frequently used to cross-link structural biopolymers however, reports of accelerated calcification of such constructs *in vivo*[12] have seen many groups seek alternative strategies for mechanically strengthening electrospun gelatin. These have included chemical cross-linking[13], coaxial spinning[14], and blending with less-brittle synthetic polymers[15-17]. Poly-ε-caprolactone (PCL), with its history of use in the body, has been previously used to this end[18].

The use of GA CL (crosslinked) electrospun gelatin and gelatin/PCL electrospun blends have not previously been reported in corneal tissue engineering. This work evaluates these biomaterial systems in terms of physiochemical and mechanical properties, and ultimately their influence on the phenotype of primary human corneal stromal cells (hCSC), derived from corneal keratocytes. We anticipate that the use of such stromal constructs to be suitable for clinical situations where the endothelium remains intact yet there is a need to support stromal replacement.

MATERIALS AND METHODS

Materials

Unless otherwise specified, materials were purchased from Sigma-Aldrich, UK.

Electrospinning

Gelatin type A (300 bloom, from porcine skin) and PCL (M_w 80,000), were dissolved in 1,1,1,3,3,3 Hexafluroisopropanol (HFIP) by stirring at 37°C overnight, to obtain polymer solutions of 8% (*w/v*). Fibrous mats were produced by electrospinning solutions of: 100% gelatin (100:0); 50% gelatin, 50% PCL (50:50); 25% gelatin, 75% PCL (25:75); and 100% PCL (0:100) in HFIP as summarised in Table 1. Electrospinning was performed though a syringe fitted with a blunt 18G stainless steel needle (0.84 mm internal diameter) attached to a syringe pump (Harvard Apparatus) set to flow rates between 0.75 ml/h and 2 ml/h, at a voltage of 15-20 kV. Fibres were collected on a grounded stainless steel plate (10 cm x 15 cm) over a working distance of 15 cm to 20 cm. After spinning a total volume of 3.5 ml/plate, fibrous mats were detached from the collector plates and placed in a vacuum oven (Heraeus Thermo Vacuum, VT6025) for 24 h to remove residual HFIP. Glass coverslips (2D controls; 400 mm^2) were immersed in 8% (*w/v*) solutions of gelatin and PCL (same ratios as above) for 1 min and solvent removed as described above.

Crosslinking Gelatin and Gelatin:PCL Scaffolds

Electrospun gelatin and gelatin: PCL mats (100:0, 50:50, 25:75, 0:100) were affixed into CellCrown™ scaffold holders (Scaffdex©, Finland) and placed in a sealed tank (8 cm x 8 cm x 5 cm), suspended 3 cm above a 1% (*v/v*) GA solution for 24 h at RT. After crosslinking, samples were immersed in 200 mM glycine at RT for 1 h to block any free residual glutaraldehyde groups.

Scanning Electron Microscopy (SEM) including Environmental SEM (ESEM)

Electrospun mats were sputter-coated with gold for 5 min at 25 mA (Leica EM SCD005, Germany) and fibre morphologies were assessed using a scanning

electron microscope (SEM; JEOL SM 1100, UK). Images were acquired of three independent batches of electrospun material each in triplicate and analysed using Image J[©] v1.47i to determine the mean fibre thickness (mean of 20 measurements for each replicate; 60 measurements in total per batch). Cross-sections of the mats were imaged by SEM to determine thickness (three individual batches; 6-10 measurements per batch). Morphology of fibrous mats (100:0 CL, and 100:0) in the hydrated state was assessed using environmental SEM (ESEM) imaging (Philips XL30 field emission gun ESEM; 3.6 Torr).

Porosity Measurements

The porosity of each scaffold was estimated using a published method[19]. In brief, scaffolds were weighed and size measured using a micrometer (Sylvac, Fowler, UK) to calculate the apparent density (Equation 1).

$$\text{apparent density} \left(\frac{\text{g}}{\text{cm}^3} \right) = \frac{\text{mat mass (g)}}{\text{mat thickness (cm)} \times \text{mat area} \left(\text{cm}^2 \right)} \tag{1}$$

Using bulk densities obtained from the literature, (gelatin 1.3 g/cm^3 [20] and PCL 1.14 g/cm^3 [21]), the ratio of the apparent and bulk densities of the materials (n=3 individual batches) were used to estimate the porosity (**Error! Reference source not found.**).

$$mat\ porosity\ (\%) = 1 - \frac{\text{mat apparent density (g/cm}^3)}{\text{material bulk density (g/cm}^3)} \times 100\% \tag{2}$$

Attenuated Total Reflectance-Fourier Transform Infrared Spectroscopy (ATR-FTIR)

Chemical analysis of the scaffolds was performed by ATR-FTIR spectroscopy (Varian 660-IR FTIR using ATR sampler accessory) over a range of 400-4000 cm^{-1}.

Assessment of gelatin and PCL content was made through comparison of the ratio of integrated peak areas (PCL ester peak at 1724 cm^{-1}; gelatin amide I peak at 1652 cm^{-1}). Pseudo-Voigt peak fitting was performed using Fityk v0.9.8 software and using corrected baselines[22].

Water Contact Angle

Water contact angle (WCA) was determined using a CAM200 instrument (KSV Instruments Ltd). Droplets of ultra-pure water (2-10 µl; 18.2 MΩ resistivity at RT) were dispensed upon scaffolds secured to a microscope slide. The Young-Laplace function was used to model and fit the droplet, using two radii of curvature. Mean and standard deviation were calculated from measurements of five different samples for each scaffold or coated glass coverslip.

Mechanical Strength

Moduli and elongation at break was measured at a rate of extension of 5 mm/min using an electromechanical universal tester (Instron 50 kN 3342, Canton, MA equipped with Series IX/S software). Rectangular sections of scaffold (300 mm x 4 mm) were mounted within a sealed acetate frame (minimum n=3 for each treatment). Effects of hydration and GA cross-linking were tested by immersion of scaffolds in PBS for 2 h at RT prior to testing. From the stress–strain curves generated, the tensile strength and Young's modulus were determined. The tensile strength was taken as the maximum stress and the Young's modulus was calculated from the linear portion of the stress–strain curve.

Human Corneal Stromal Cell Isolation, Expansion and Culture on Scaffolds

Donor human corneas deemed unsuitable for transplantation were acquired from the Manchester Eye Bank following consent obtained from the donors or their relatives and anonymization. Research was approved by the local ethics research committee (07/H0403/140) and in accordance with the tenets of the Declaration of Helsinki. Three independent patient donors (n=3; in order to take into account patient to patient variability) were used for this study. Cells were extracted from corneoscleral rims by collagenase digestion as previously described[23]. Cells were cultured in Dulbecco's Modified Eagle's Medium (DMEM), supplemented with 10% (*v/v*) foetal calf serum (FCS), 0.2 mM L-glutamine and 1% (*v/v*) antibiotic-antimycotic (ABAM,10,000 units/ml penicillin, 10 mg/ml streptomycin; 25 mg/ml amphotericin B; Fibroblast (F) medium). For seeding onto scaffolds, the electrospun mats were mounted into CellCrown scaffold holders (80mm^2) and sterilized using a 254 nm UVP XX-15W UV lamp for 20 min and soaked in 1% (*v/v*) ABAM solution for 8 h, followed by pre-soaking in F medium for 24 h. hCSC (passage 2) were seeded onto scaffolds at a density 2×10^4 cells/cm^2 in F medium. To drive hCSCs towards a keratocyte phenotype, hCSC were cultured in DMEM/F12 (Lonza, Belgium) supplemented with 1% (*v/v*) ABAM, 1 μg/ ml human insulin and 1 mM L-Ascorbic acid-2-phosphate; Keratocyte (K) medium). Culture, expansion, and differentiation of hCSCs followed methods previously described[23-24]. Cells were expanded and used in all experiments at passage 2-3.

Analysis of Cell-Scaffold Interactions

PrestoBlue® assays (Life Technologies, UK) were performed on days 1, 3, 6 and 12 according to the manufacturer's protocol to assess cell viability. In brief, scaffolds

were washed with Hanks Buffered Saline Solution (HBSS) and incubated with 10% (*v/v*) PrestoBlue® stock diluted in HBSS for 30 min at 37°C. Fluorescence at excitation 560nm/emission 590 nm was measured using a fluorometric plate reader (Tecan Infinite 1000, UK). Transparency of constructs seeded with 1×10^5 cells/cm^2 hCSC were evaluated by placing over laminated sheets of text (letter A) after 12 d in culture and compared to acellular controls (images captured using an EOS 100D digital camera; Canon, Chichibu, Japan).

Reverse-Transcription-quantitative Polymerase Chain Reaction (RT-qPCR)

For gene expression, hCSC were seeded on scaffolds at a density of 1×10^5 cells/cm^2 and cultured for 12 d in K medium. RNA extraction, cDNA synthesis and qPCR were performed as previously described[23]. Quantitative PCR reactions were performed with a 2 µL cDNA volume using inventoried Taqman Assays (Applied Biosystems, Life Technologies): *GAPDH* (Hs99999905_m1), *CD34* (Hs00990732_m1), *ALDH3A1* (Hs00964880), *ACTA2* (Hs00426835_g1) and *THY1* (Hs0017816_m1). Amplification was performed using an AB7500 quantitative PCR machine (Applied Biosystems) and analysed using AB7500 SDS v.2.0 software. Relative expression levels were determined using the $2^{-\Delta\Delta(CT)}$ method and normalized to readings of *GAPDH*. RNA was isolated from hCSC cultured on triplicate samples of each scaffold and pooled; three separate experiments were performed to generate n=3 data.

Sectioning and Immunostaining of Constructs

Cell-seeded scaffolds were fixed in 4% (*w/v*) paraformaldehyde at room temperature (RT) for 20 min. Samples were dehydrated though a series of graded alcohol solutions in a tissue processor (Leica TP1020) and paraffin-embedded. Sections of 8

μm were cut (Leica RM 2165 microtome) and placed onto microscope slides. Samples were deparaffinised in xylene, rehydrated in a series of graded alcohol solutions, and antigen retrieval achieved in a pH 6.0 sodium citrate buffer at 95°C for 60 min. Immunofluorescent staining was performed as described previously[23] using the antibodies detailed in Table 2. Samples were counterstained with 4',6-diamidino-2-phenylindole (DAPI; 1:200,000), mounted in fluorescent mounting medium (Dako, UK) and imaged under an Olympus BX51 upright microscope using the associated Olympus Cell^F software.

Statistical analysis

Results are expressed as mean±standard error of the mean (SEM) unless otherwise described. Statistical significance for material characterization studies was estimated by one-way ANOVA tests in GraphPad Prism v6.01 followed by Tukey post-hoc test to compare groups. Cell data was analysed by two-way ANOVA followed by a Bonferroni post-hoc test. Levels of significance were expressed as p values versus the control (*$p < 0.05$, **$p < 0.01$, ***$p < 0.001$).

RESULTS

Fibrous scaffolds composed of gelatin and PCL were fabricated

SEM images showed gelatin scaffolds (100:0) were composed of ribbon-like fibres (Figure 1A), distinct from the rounded fibres observed for PCL (0:100) scaffolds (Figure 1D). Both 50:50 and 25:75 scaffolds showed signs of ribboning within the matrix (Figure 1B & C). Characterisation of scaffolds in terms of fibre and scaffold thickness, porosity and WCA is presented in Table 3. Fibre thickness was notably

larger in the 100:0 scaffolds (2.20μm ± 1.02 μm), relative to the other scaffolds containing PCL (0.89 ± 0.58 to 0.62 ± 0.47 μm). Scaffold thicknesses for all formulations were relatively consistent (62 - 76 μm).

WCA of the electrospun scaffolds showed a marked difference between scaffolds made from the pure materials (100:0 - 40.3° ± 5.46 and 0:100 - 85.4° ± 6.9). However, no relationship between material composition and WCA was observed in scaffolds generated from blends of the two materials (50:50 55.5° ± 19.4 and 25:75 – 44.5° ± 8.9). In assessing the porosity of the scaffolds, no relationship was observed between material composition and porosity (100:0 - 65.6%; 50:50 73.3%; 25:75 - 63.4%; 0:100 - 88.75% porosity).

ATR-FTIR was used to confirm the chemical composition of the scaffolds. Figure 1E displays the key region of interest presenting the percentage transmittance for each scaffold offset by 10%. Gelatin related amide bands at 1652 cm^{-1} (amide I) and 1542 cm^{-1} (amide II) were observed in all gelatin containing scaffolds (100:0, 50:50 and 25:75). PCL related ester bands were confirmed in 0:100, 25:75, 50:50 scaffolds at 1724 cm^{-1} (carbonyl stretching), 1293 cm^{-1} (C–O and C–C stretching) and 1240 cm^{-1} (asymmetric C-O-C stretching). To assess the ratio of ester to amide, FTIR peaks at 1724cm^{-1} and 1652 cm^{-1} were integrated (Figure 1F). The 50:50 and 25:75 scaffolds were observed to have distinctly different ratios of the two bands (50:50 - 0.46; 25:75 – 0.32). To enhance the mechanical properties (and prevent dissolution of the gelatin in later cell culture studies) of 100:0 gelatin:PCL scaffolds, samples were CL over GA vapour for 16 h. SEM images of the 100:0 scaffold before (Figure 2A) and after cross-linking (Figure 2B), show a distinct change in the fibrous morphology of the

scaffold and as a consequence, fibre diameters in the CL scaffold were not measurable. ATR-FTIR analysis of the scaffolds before and after GA cross-linking shows an increase in transmittance percentage at 1450 cm^{-1} corresponding to an aldimine group (Figure 2C). After cross-linking, the scaffolds became notably less porous (100:0 - 65.6%; 100:0 CL - 33.7%), however there was little difference observed between scaffold thickness (100:0 - 75.03 µm ± 16.1; 100:0 CL - 70.82 µm ± 10.05) (Figure 2D). ESEM images were acquired of both CL gelatin (100:0 CL) and PCL (0:100) scaffolds in a partially hydrated state (Figure 2E & F) confirming a fibrous structure.

Hydration influences the mechanical properties of the scaffolds

Tensile testing of scaffolds with four different ratios of gelatin:PCL, before and after cross-linking for all samples and following hydration is shown in Figure 3. In the dry state, the tensile modulus (E) decreased with increasing PCL content ranging from 136 MPa ± 61 (100:0) down to 15 MPa ± 5 (0:100) (Figure 3A). In the hydrated state, this trend reversed and the modulus increased with increasing PCL content (Figure 3B). The 0:100 and 25:75 scaffolds recorded similar moduli in both wet and dry states (**Dry** 25:75 - 40.6 MPa ± 15.2; 0:100 - 15.5 MPa ± 2.3; **Wet** 25:75 - 39MPa ± 8; 0:100 - 33MPa ± 7. The 50:50 and 100:0 formulations exhibited significantly lower moduli when hydrated, with 100:0 scaffolds possessing a modulus of 136 MPa ± 61 whilst dry, but when wet the material was too fragile to measure. The moduli of the 50:50 scaffolds changed from an average of 57 MPa ± 18 whilst dry to 4 MPa ± 0.2 once hydrated.

Cross-linking of the 100:0 scaffold resulted in the increase of the Young's modulus significantly in the dry testing regime (Figure 3A), with increasing modulus from 136 MPa ± 6 to 1858 MPa ± 47 (CL). Non-CL100:0 scaffolds in the hydrated state could not be tested due to a loss of integrity of the scaffold after hydration (Figure 3B). Cross-linking had little effect on the mechanical properties of the 50:50, 75:25 and 0:100 scaffolds in both dry and hydrated states. When compared to full thickness cornea tensile testing (3 - 13 MPa[26]), 50:50 scaffolds appeared to most closely fit the observed range with a modulus of 5.5 MPa ± 0.8. Elongation at break in the dry testing regime increased with increasing PCL content ranging from 0.014 ± 0.003 mm/mm (100:0) up to 0.229 ± 0.100 mm/mm (0:100; Figure 3C). PCL 0:100 scaffolds were able to reach over 20% extension before failure, irrespective of hydration (Figure 3C & D). Elongation at break of gelatin containing scaffolds was seen to increase with hydration; 0.066 ±0.044 mm/mm when dry (50:50) to 0.386 ± 0.082 mm/mm when hydrated (Figure 3D).

Fibrous scaffolds were biocompatible for hCSC with PCL scaffolds containing gelatin supporting a quiescent keratocyte phenotype

The biocompatibility of 100:0 CL scaffolds along with 50:50; 25:75 and 0:100 scaffolds were compared in terms of hCSC adhesion and proliferation on the scaffolds. Over a 5 h period, significantly more hCSC adhered to 100:0 CL scaffolds than the 0:100 scaffolds observed through a difference in relative fluorescence of 514 ± 51 RFU for cells cultured on 100:0 CL relative to 277 ± 37 for cells on 0:100 scaffolds (PrestoBlue®; Figure 4A). However, there were no significant differences between hCSC adherence to 100:0 CL, 50:50 or 25:75 scaffolds (Figure 4A). hCSC

were able to proliferate over a 12 day period on all four electrospun scaffolds at similar rates (Figure 4B).

Assessment of the effects of surface chemistry on adhesion, without potential differences in topography, was performed using glass coverslips dip-coated in HFIP solutions of each of the formulations (confirmed by WCA measurements; Figure 4C). A similar hCSC adhesion experiment was performed (Figure 4D) and similar trends were observed on the coated glass coverslips as observed on the fibrous scaffolds. A difference in relative fluorescence determined in the PrestoBlue® assay of 994 ± 103 for cells cultured on 100:0 CL coated glass coverslips was observed relative to 501 ± 54 for cells on 0:100 coated glass coverslips. However, in contrast to the data generated with the fibrous scaffolds, the 100:0 CL coated glass also supported significantly higher hCSC adhesion than 50:50 or 25:75 coated glass.

qPCR was used to assess gene expression of two markers of the quiescent (non-scarring) keratocyte phenotype, ALDH3A1 and CD34, and two markers of the activated (scarring) fibroblast phenotype, *ACTA2* (α-SMA) and *THY1* (CD90). Gene expression data was compared to cells cultured on the gelatin scaffold rather than the native cornea stomal tissue as the cells had been cultured *in vitro* prior to these experiments. Overall relative gene expression responses to the electrospun substrates were small with a 4-fold increase being the greatest response observed in all experiments (Figure 5A). Statistically significant increases in *ALDH* expression were observed in hCSC cultured on the both 50:50 and 25:75 scaffolds relative to 100:0 CL. hCSC cultured on 0:100 scaffolds expressed significantly more *THY1* than

those on 100:0 CL. To assess the direct effect of cross-linking on the phenotype of hCSC, cells were cultured on 50:50 scaffolds with and without cross-linking and phenotype was assessed (Figure 5B).

Scaffolds 50:50 and 50:50 CL differed little in terms of *CD34* and *THY1* expression in this experiment. *ACTA2* expression was the largest and only statistically significant difference recorded which was increased when cells were cultured on CL samples (Figure 5B). This phenomenon was explored further though assessing protein expression by immunofluorescence (Figure 6). Cells were clearly situated in a layer on top of the scaffolds and hCSC cultured on 50:50 scaffolds which had not been CL were seen to express higher levels of CD34 and CD90. *α-SMA* appears to be expressed to a higher degree by hCSC cells cultured on 50:50 CL scaffolds. Macroscopic images captured after 12 d culture with or without hCSCs in K medium showed that 100:0 CL scaffolds were more transparent than any PCL containing scaffold (Figure 7). No differences were observed between the other scaffold types with or without hCSC.

DISCUSSION

A global shortage of corneal donor tissue, coupled with increasing levels of adoption of deep anterior lamellar keratoplasty (DALK) has resulted in a need for partial thickness corneal tissue grafts[1].The development of tissue-engineered stromal replacements hold promise to supplement the donor tissue pool in addition to producing standardized constructs. We anticipate that the use of such stromal constructs to be suitable for DALK procedures used in clinical situations where the endothelium remains intact yet there is a need to support stromal replacement. Such constructs would allow the surgeon flexibility to replace the stroma layer by layer

depending on the depth of the injury. Re-epithelialization would then occur from the patient's own limbal stem cell reserve or in combination with limbal stem cell transplantation.

Our approach proposes the use of polymeric platforms, produced by electrospinning, as biomimetic constructs for corneal tissue regeneration. More specifically, this paper compares the attributes of gelatin and PCL electrospun blends relative to chemically CL gelatin as a novel way to produce suitable candidates for stromal replacement. This work represents the first time an electrospun composite of synthetic and natural polymers has been evaluated as a candidate material for corneal stromal tissue engineering.

Gelatin was chosen on account of its bioactivity, biodegradability, non-antigenicity, current use in clinical applications, stability during electrospinning and commercial availability at low cost[10-11]. PCL was chosen as an alternative to glutaraldehyde cross-linking to provide strength to gelatin based scaffolds as it is biocompatible, biodegradable and has been extensively explored for applications in tissue engineering[18]. The longer degradation time of PCL (anticipated to be 6-12 months based on our knowledge of PCL-based scaffolds) was attractive for the production of fibrous materials to contrast our experience with other polymers, such as PLGA, which rapidly lose integrity when wet. The lack of transparency of PCL was not considered an issue for clinical applications as polymer degradation and tissue remodelling would allow for restoration of sight; we show that the scaffolds are opaque and this would be sufficient for perception of light/dark following surgery. We

therefore wanted to explore the novel application of PCL-gelatin blended scaffolds in ophthalmology.

In optimised electrospinning conditions, gelatin produced ribbon-like fibres upon deposition in line with previous reports[17, 28], whereas rounded fibres were achieved in all PCL containing scaffolds[29-30]. Fibre diameter of gelatin based scaffolds was seen to decrease and the WCA increased through introducing PCL. Other investigations of gelatin:PCL blends have not reported such fibre diameter trends although the WCA data agrees with other work[27, 29-30]. All these studies, including our findings reported here, produced fibres an order of magnitude greater than the collagen fibrils found *in vivo* (31 to 34 nm) but are similar in diameter to lamellae structures, which are approximately 1 to 2 μm thick[6,40]. The distinct material compositions of the different gelatin:PCL blends were successfully validated though ATR-FTIR. The presence of both amide and ester bands in the 25:75 and 50:50 gelatin:PCL scaffolds confirmed that both materials were present at the surface of the scaffolds, as described in the literature[39,40].

The high solubility of gelatin in aqueous solutions meant that cross-linking was required. Cross-linking of 100:0 gelatin scaffolds with GA resulted in the webbing of individual fibres resulting in a significant drop in the porosity of the scaffold. Uniaxial tensile testing showed that GA cross-linking of 100:0 scaffolds significantly increased the modulus and elongation at break. The effect of GA treatment on the 50:50 and 25:75 scaffolds was not significant, suggesting that the mechanical properties of PCL dominate in this system. All scaffolds in the hydrated state were capable of withstanding the same level of strain before failure. The Young's modulus of the

healthy human cornea has been previously reported to be *ca.* 3 MPa[26,31] which corresponds to the measured moduli of the hydrated 50:50 and 100:0 CL scaffolds. As the concentration of PCL increased, the tensile moduli of the scaffolds decreased as seen in other studies where gelatin is included in the blend[16-17,39]. In the hydrated state, this trend was seen to reverse. The moduli of the gelatin scaffolds in both 100:0 CL and 50:50 compositions decreased upon hydration, when brittle fibres swelled to become hydrogel-like[28]. Mechanical testing of gelatin-based electrospun scaffolds in the hydrated state has not been previously reported. The degradation of the scaffolds produced was not studied here (although they were visually intact for up to 21 days) and would be a next step in further evaluating these scaffolds for clinical applications.

For application in corneal stroma repair, it was important to evaluate the biocompatibility of the scaffolds with hCSC. The cells adhered to all scaffolds of various compositions with cell adhesion highest on the gelatin based scaffolds suggesting that there was insufficient, if any, GA remaining to be detrimental to the cells. Experiments on 2D controls of the same formulations demonstrated that chemistry was the dominant effect on cell adhesion in these studies (rather than fibre morphology). *ALDH3A1*[32-33] and CD34[34-36] are important markers of keratocytes *in vivo* alongside keratocan expression[25,37]. The expression of CD90 (gene name *THY1*) and α-SMA (gene name *ACTA2*) are characteristic of a less desirable myofibroblastic phenotype that leads to scarring[25]. Our data suggested that 50:50 and 25:75 scaffolds offer a substrate more supportive of the keratocyte phenotype, with decreased *α-SMA* and increased CD34 and *ALDH3A1* expression. Previous work published by our laboratories have compared similar isolated cells cultured *in vitro* to those resident in the native cornea. Compared to the native cornea,

ALDH3A1, CD34 and ACTA2 were significantly down regulated and THY1 was significantly upregulated[25]. This suggests that when cultured *in vitro*, the whole population of cells do not differentiate to the keratocyte phenotype warranting further optimisation of scaffold morphology and *in vitro* culture conditions. In addition, comparison of the expression of these markers from *in vitro* cultured cells with those expressed *in vivo* is further required.

In considering clinical therapies for the cornea, the refractive index of the scaffolds is an important factor[38,39]. Gelatin 100:0 CL scaffolds demonstrated a higher transmittance of visible light and this increased following culture with hCSC suggesting remodelling of the extracellular matrix. Longer culture studies are required to assess matrix remodelling and degradation in the gelatin-PCL scaffolds in relation to transparency. Further optimisation of the fibre diameter to allow penetration of the cells throughout the scaffold, whilst supporting the quiescent (non-scarring) cell phenotype, would also be a focus of future work. Future *in vivo* studies would also be required to ascertain the ability of these scaffolds to support the quiescent (non-scarring) keratocyte phenotype in the longer term and ultimately the restoration of visual acuity. In conclusion, we have demonstrated for the first time that hCSC cultured on blended gelatin-PCL scaffolds adopt a therapeutically desirable quiescent phenotype illustrating their suitability as future corneal repair materials.
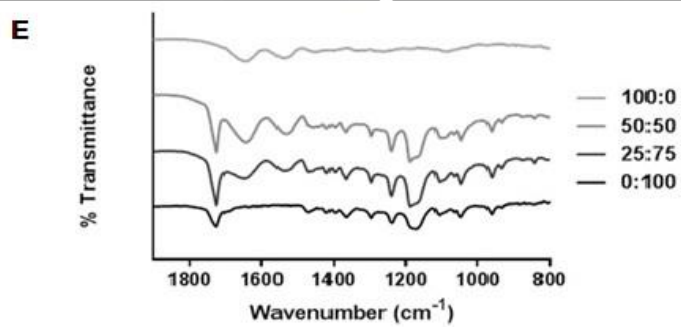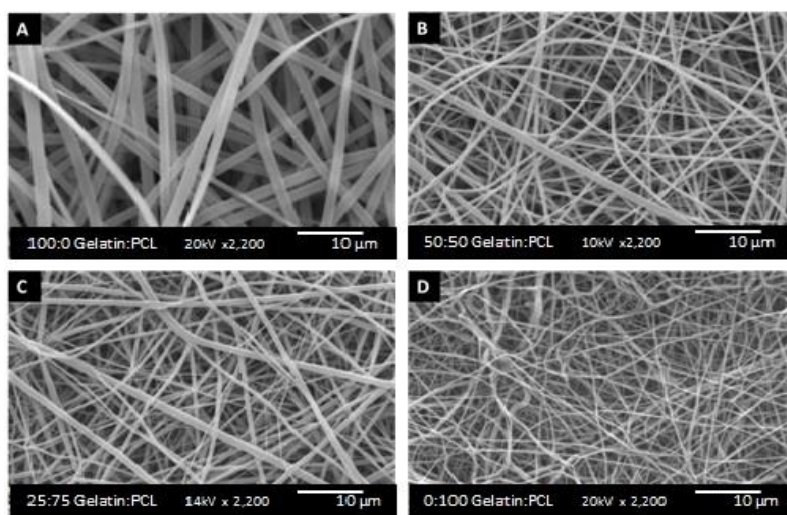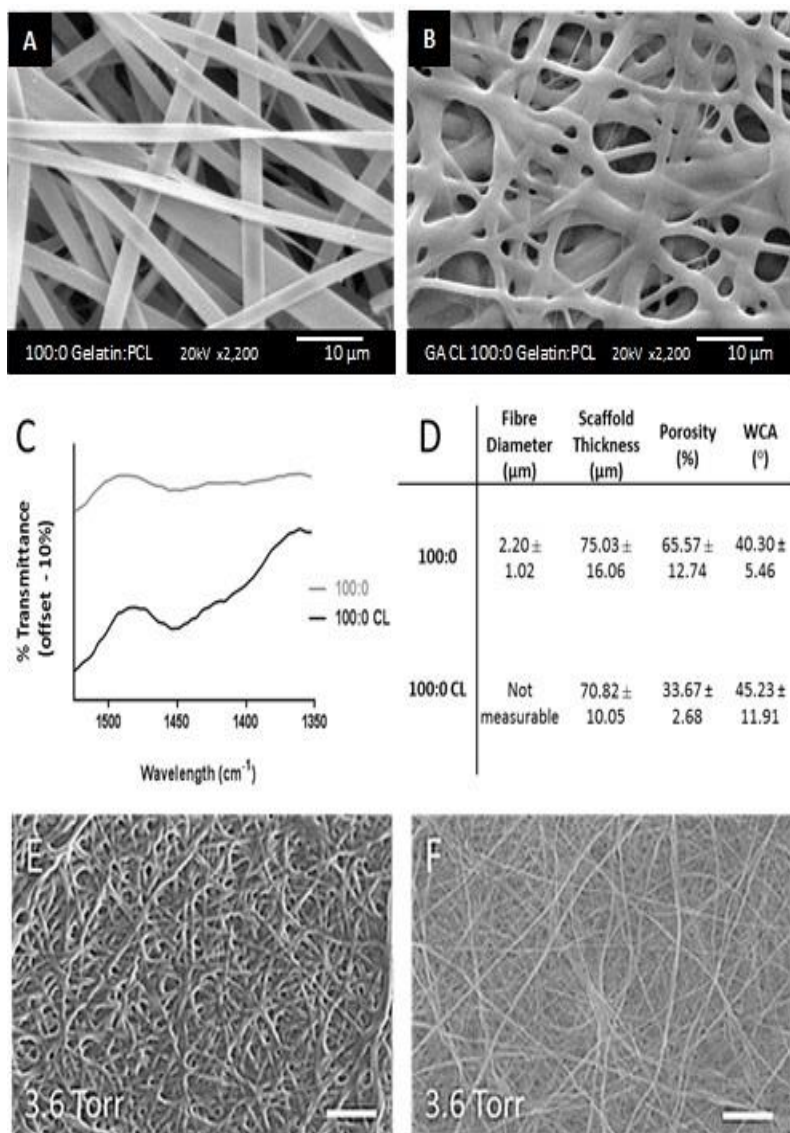
REFERENCES

1. Keenan TDL, Carley F, Yeates D, Jones MNA, Rushton S, Goldacre MJ. Trends in corneal graft surgery in the UK. British Journal of Ophthalmology 2011;95(4):468-472.
2. Li J, Yu L, Deng Z, Wang L, Sun L, Ma H, Chen W. Deep anterior lamellar keratoplasty using acellular corneal tissue for prevention of allograft rejection in high-risk corneas. Am J Ophthalmol 2011;152(5):762-70 e3.
3. MacIntyre R, Chow SP, Chan E, Poon A. Long-term outcomes of deep anterior lamellar keratoplasty versus penetrating keratoplasty in Australian keratoconus patients. Cornea 2014;33(1):6-9.
4. Lagali N, Fagerholm P, Griffith M. Biosynthetic corneas: prospects for supplementing the human donor cornea supply. Expert Rev Med Devices 2011;8(2):127-30.
5. Jester JV, Moller-Pedersen T, Huang J, Sax CM, Kays WT, Cavangh HD, Petroll WM, Piatigorsky J. The cellular basis of corneal transparency: evidence for 'corneal crystallins'. J Cell Sci 1999;112 (Pt 5):613-22.
6. Ruberti JW, Zieske JD. Prelude to corneal tissue engineering - gaining control of collagen organization. Prog Retin Eye Res 2008;27(5):549-77.
7. Ortega I, Ryan AJ, Deshpande P, MacNeil S, Claeyssens F. Combined microfabrication and electrospinning to produce 3-D architectures for corneal repair. Acta Biomater 2013;9(3):5511-20.
8. Rho KS, Jeong L, Lee G, Seo BM, Park YJ, Hong SD, Roh S, Cho JJ, Park WH, Min BM. Electrospinning of collagen nanofibers: effects on the behavior of normal human keratinocytes and early-stage wound healing. Biomaterials 2006;27(8):1452-61.
9. Li M, Mondrinos MJ, Gandhi MR, Ko FK, Weiss AS, Lelkes PI. Electrospun protein fibers as matrices for tissue engineering. Biomaterials 2005;26(30):5999-6008.
10. Zeugolis DI, Khew ST, Yew ES, Ekaputra AK, Tong YW, Yung LY, Hutmacher DW, Sheppard C, Raghunath M. Electro-spinning of pure collagen nano-fibres - just an expensive way to make gelatin? Biomaterials 2008;29(15):2293-305.
11. Rose JB, Pacelli S, Haj AJE, Dua HS, Hopkinson A, White LJ, Rose F. Gelatin-Based Materials in Ocular Tissue Engineering. Materials (Basel) 2014;7(4):3106-3135.
12. Schoen FJ, Levy RJ. Calcification of tissue heart valve substitutes: progress toward understanding and prevention. Ann Thorac Surg 2005;79(3):1072-80.
13. Skotak M, Ragusa J, Gonzalez D, Subramanian A. Improved cellular infiltration into nanofibrous electrospun cross-linked gelatin scaffolds templated with micrometer-sized polyethylene glycol fibers. Biomed Mater 2011;6(5):055012.
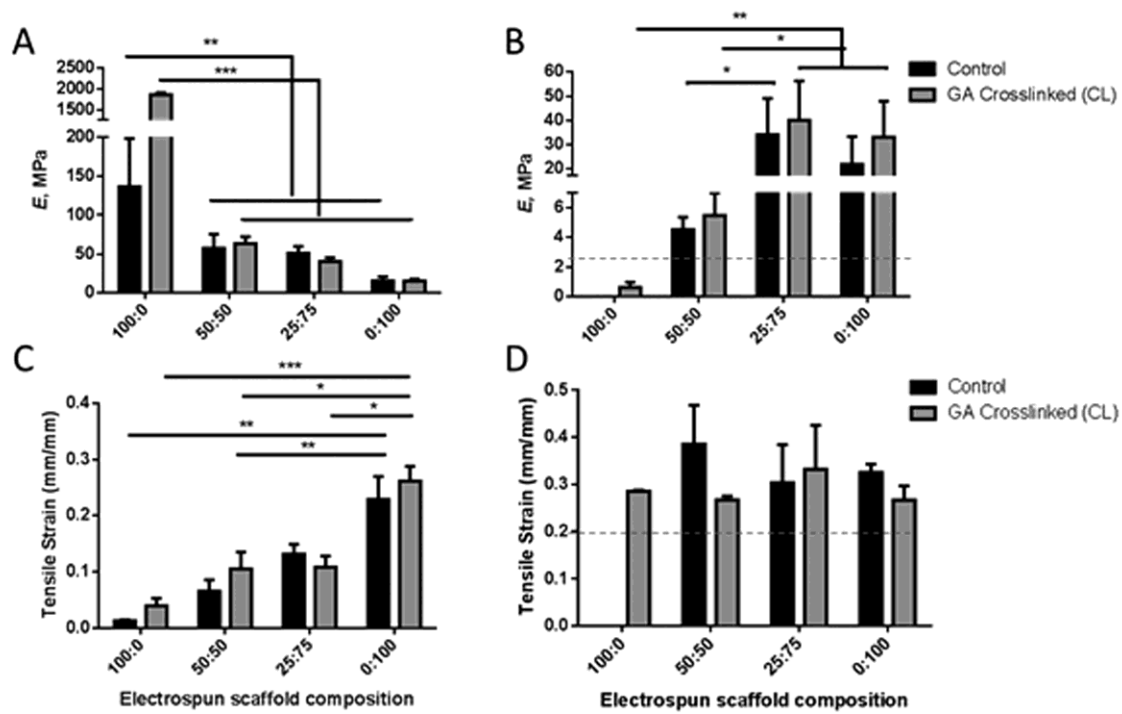
14. Zhao P, Jiang H, Pan H, Zhu K, Chen W. Biodegradable fibrous scaffolds composed of gelatin coated poly(epsilon-caprolactone) prepared by coaxial electrospinning. J Biomed Mater Res A 2007;83(2):372-82.

15. Alvarez-Perez MA, Guarino V, Cirillo V, Ambrosio L. Influence of gelatin cues in PCL electrospun membranes on nerve outgrowth. Biomacromolecules 2010;11(9):2238-46.

16. Zhang Y, Ouyang H, Lim CT, Ramakrishna S, Huang ZM. Electrospinning of gelatin fibers and gelatin/PCL composite fibrous scaffolds. J Biomed Mater Res B Appl Biomater 2005;72(1):156-65.

17. Lee J, Tae G, Kim YH, Park IS, Kim SH, Kim SH. The effect of gelatin incorporation into electrospun poly(L-lactide-co-epsilon-caprolactone) fibers on mechanical properties and cytocompatibility. Biomaterials 2008;29(12):1872-9.

18. Cipitria A, Skelton A, Dargaville TR, Dalton PD, Hutmacher DW. Design, fabrication and characterization of PCL electrospun scaffolds-a review. Journal of Materials Chemistry 2011;21(26):9419-9453.

19. Zhu X, Cui W, Li X, Jin Y. Electrospun fibrous mats with high porosity as potential scaffolds for skin tissue engineering. Biomacromolecules 2008;9(7):1795-801.

20. Chong EJ, Phan TT, Lim IJ, Zhang YZ, Bay BH, Ramakrishna S, Lim CT. Evaluation of electrospun PCL/gelatin nanofibrous scaffold for wound healing and layered dermal reconstitution. Acta Biomater 2007;3(3):321-30.

21. Jahani H, Kaviani S, Hassanpour-Ezatti M, Soleimani M, Kaviani Z, Zonoubi Z. The effect of aligned and random electrospun fibrous scaffolds on rat mesenchymal stem cell proliferation. Cell J 2012;14(1):31-8.

22. Wojdyr M. Fityk: a general-purpose peak fitting program. Journal of Applied Crystallography 2010;43(5 Part 1):1126-1128.

23. Sidney LE, Branch MJ, Dua HS, Hopkinson A. Effect of culture medium on propagation and phenotype of corneal stroma–derived stem cells. Cytotherapy 2015;17(12):1706-1722.

24. Musselmann K, Alexandrou B, Kane B, Hassell JR. Maintenance of the keratocyte phenotype during cell proliferation stimulated by insulin. J Biol Chem 2005;280(38):32634-9.

25. Sidney LE, Hopkinson A. Corneal keratocyte transition to mesenchymal stem cell phenotype and reversal using serum-free medium supplemented with fibroblast growth factor-2, transforming growth factor-beta3 and retinoic acid. J Tissue Eng Regen Med 2018;12(1):e203-e215.

26. Merrett K, Fagerholm P, McLaughlin CR, Dravida S, Lagali N, Shinozaki N, Watsky MA, Munger R, Kato Y, Li F and others. Tissue-engineered recombinant human collagen-based corneal substitutes for implantation: performance of type I versus type III collagen. Invest Ophthalmol Vis Sci 2008;49(9):3887-94.

27. Nam J, Huang Y, Agarwal S, Lannutti J. Materials selection and residual solvent retention in biodegradable electrospun fibers. Journal of Applied Polymer Science 2007;107(3):1547-1554.

28. Nguyen T, Lee B. Fabrication and characterization of cross-linked gelatin electro-spun nano-fibers. J Biomed Sci and Eng 2010;3:1117-1124

29. Ghasemi-Mobarakeh L, Prabhakaran MP, Morshed M, Nasr-Esfahani MH, Ramakrishna S. Electrospun poly(epsilon-caprolactone)/gelatin nanofibrous scaffolds for nerve tissue engineering. Biomaterials 2008;29(34):4532-9.

30. Guarino V, Alvarez-Perez M, Cirillo V, Ambrosio L. hMSC interaction with PCL and PCL/gelatin platforms: A comparative study on films and electrospun membranes. Journal of Bioactive and Compatible Polymers 2011;26(2):144-160.
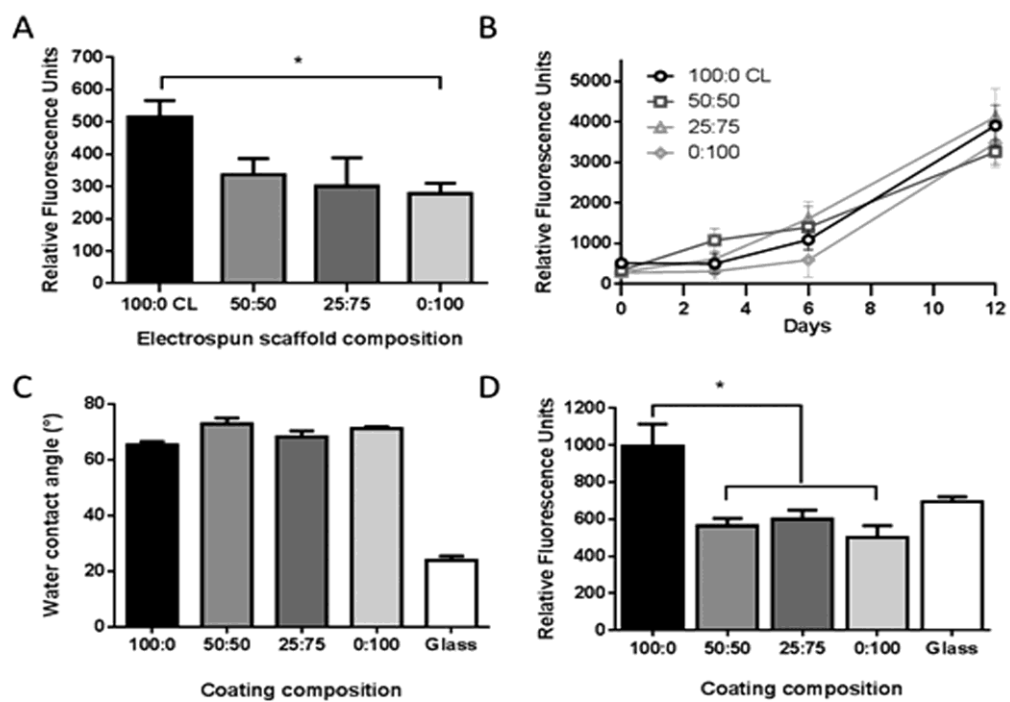
31. McKee CT, Last JA, Russell P, Murphy CJ. Indentation versus tensile measurements of Young's modulus for soft biological tissues. Tissue Eng Part B Rev 2011;17(3):155-64.

32. Pei Y, Reins RY, McDermott AM. Aldehyde dehydrogenase (ALDH) 3A1 expression by the human keratocyte and its repair phenotypes. Exp Eye Res 2006;83(5):1063-73.

33. Du Y, Funderburgh ML, Mann MM, SundarRaj N, Funderburgh JL. Multipotent stem cells in human corneal stroma. Stem Cells 2005;23(9):1266-75.

34. Sidney LE, Branch MJ, Dunphy SE, Dua HS, Hopkinson A. Concise review: evidence for CD34 as a common marker for diverse progenitors. Stem Cells 2014;32(6):1380-9.

35. Sidney LE, McIntosh OD, Hopkinson A. Phenotypic Change and Induction of Cytokeratin Expression During In Vitro Culture of Corneal Stromal Cells. Invest Ophthalmol Vis Sci 2015;56(12):7225-35.

36. Joseph A, Hossain P, Jham S, Jones RE, Tighe P, McIntosh RS, Dua HS. Expression of CD34 and L-selectin on human corneal keratocytes. Invest Ophthalmol Vis Sci 2003;44(11):4689-92.

37. Park SH, Kim KW, Chun YS, Kim JC. Human mesenchymal stem cells differentiate into keratocyte-like cells in keratocyte-conditioned medium. Exp Eye Res 2012;101:16-26.

38. Wu J, Du Y, Watkins SC, Funderburgh JL, Wagner WR. The engineering of organized human corneal tissue through the spatial guidance of corneal stromal stem cells. Biomaterials 2012;33(5):1343-52.

39. Tonsomboon K, Oyen ML. Composite electrospun gelatin fiber-alginate gel scaffolds for mechanically robust tissue engineered cornea. J Mech Behav Biomed Mater 2013;21:185-94.

40. Winkler M, G Shoa,Y Xie, SJ Petsche, PM Pinsky, T Juhasz, DJ Brown, JV Jester. Three-Dimensional Distribution of Transverse Collagen Fibers in the Anterior Human Corneal Stroma. Invest Ophthalmol Vis Sci. 2013; 54(12): 7293–7301.

A — 100:0 Gelatin:PCL 20kV x2,200 10 μm
B — 50:50 Gelatin:PCL 10kV x2,200 10 μm
C — 25:75 Gelatin:PCL 14kV x 2,200 10 μm
D — 0:100 Gelatin:PCL 20kV x 2,200 10 μm

E

% Transmittance vs Wavenumber (cm^{-1})

— 100:0
— 50:50
— 25:75
— 0:100

F Wavenumber	Electrospun scaffold composition			
	100:0	50:50	25:75	0:100
1652 cm^{-1}	1.00	0.46	0.32	0
1724 cm^{-1}	0	0.54	0.68	1.00

A	B
100:0 Gelatin:PCL 20kV x2,200 10 μm	GA CL 100:0 Gelatin:PCL 20kV x2,200 10 μm

C

% Transmittance (offset - 10%)

Wavelength (cm⁻¹)

— 100:0
— 100:0 CL

D

	Fibre Diameter (μm)	Scaffold Thickness (μm)	Porosity (%)	WCA (°)
100:0	2.20 ± 1.02	75.03 ± 16.06	65.57 ± 12.74	40.30 ± 5.46
100:0 CL	Not measurable	70.82 ± 10.05	33.67 ± 2.68	45.23 ± 11.91

E	F
3.6 Torr	3.6 Torr

	DAPI	ALDH3A1	α-SMA	CD34	CD90
50:50	A	B	C	D	E
50:50	F	G	H	I	J
50:50 CL	K	L	M	N	O
50:50 CL	P	Q	R	S	T

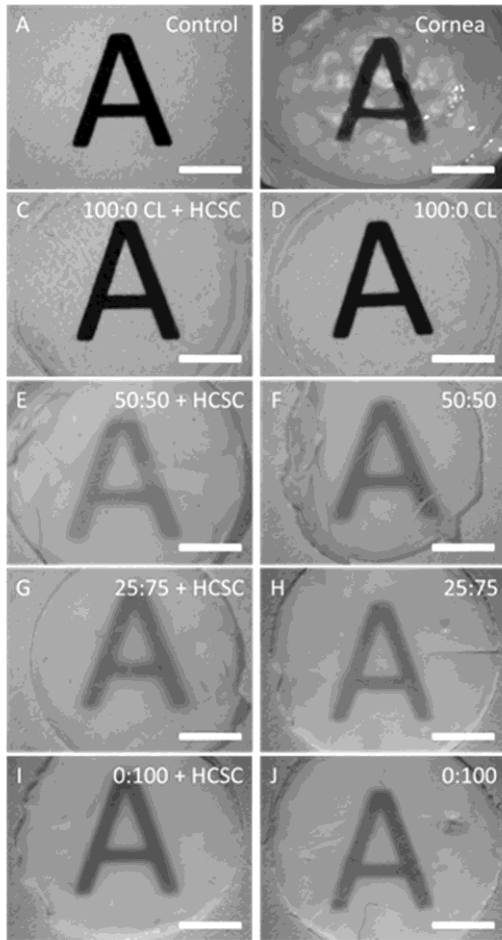U   V   W   X

50:50   **50:50 CL**

Table 1. Electrospinning conditions for fabrication of gelatin:PCL electrospun scaffolds

Polymer Blend (Gelatin : PCL)	Polymer Conc. (w/w)	Working Distance (mm)	Working Voltage (kV)	Flow Rate (ml/h)	Spinning Volume (ml)	Spinning Time (min)
100 : 0	8.0%	150	12.5	0.75	3.5	280
50 : 50	8.0%	150	15	2.0	3.5	105
25 : 75	8.0%	150	15	0.8	3.5	265
0 : 100	8.0%	200	20	0.8	3.5	265

Table 2. Antibodies used for immunocytochemistry

Antibody	Supplier	Dilution
Primary Antibodies		
polyclonal rabbit anti-*ALDH3A1*	Abcam	1:100
monoclonal mouse anti-*α-SMA* clone 1A4	Abcam	1:200
polyclonal rabbit anti-*CD34*	Santa Cruz	1:50
monoclonal mouse anti-*CD90* clone AF-9	Abcam	1:200
Secondary Antibodies		
donkey anti-mouse Alexa-Fluor 594	Life Technologies	1:300
donkey anti-rabbit Alexa Fluor 488	Life Technologies	1:300

Table 3. Characterisation of scaffolds, describing fibre diameter, scaffold thickness, porosity and water contact angle (WCA). All measurements are represented by mean±SD (n = 3)

Polymer Blend (Gelatin:PCL)	Fibre Thickness (µm)	Scaffold Thickness (µm)	Porosity (%)	WCA (°)
100:0	2.20 ± 1.02	75.03 ± 16.06	65.57 ± 12.74	40.30 ± 5.46
50:50	0.89 ± 0.58	73.62 ± 10.05	73.28 ± 19.23	55.51 ± 19.38
25:75	0.63 ± 0.22	76.00 ± 12.21	63.94 ± 16.89	44.47 ± 8.92
0:100	0.62 ± 0.47	62.15 ± 22.44	88.75 ± 3.31	85.37 ± 6.87